DISCOVERY

58(322), October 2022

3D Quantitative structure–activity relationship to predict the anti-malarial activity in a set of Cycloguanil Analogs

Olalekan A. Agede[1,2,5*], Mathew O. Bojuwoye[1], Adeniyi F. Adenike[3], Olugbenga A. Mokuolu[4,5], Catherine O. Falade[6,7]

To Cite:
Agede OA, Bojuwoye MO, Adenike AF, Mokuolu OA, Falade CO. 3D Quantitative structure–activity relationship to predict the anti-malarial activity in a set of Cycloguanil Analogs. *Discovery*, 2022, 58(322), 1097-1108

Author Affiliation:
[1]Department of Medicine, University of Ilorin Teaching Hospital, Ilorin, Nigeria
[2]Department of Pharmacology and Therapeutics, Division of Clinical Pharmacology and Therapeutics, University of Ilorin, Ilorin, Nigeria
[3]Department of Mathematics, University of Ilorin, Ilorin, Nigeria
[4]Department of Paediatrics and Child Health, University of Ilorin and University of Ilorin Teaching Hospital, Ilorin, Nigeria
[5]Malaria Research Center, University of Ilorin Teaching Hospital, Ilorin, Nigeria
[6]Department of Pharmacology and Therapeutics, Division of Clinical Pharmacology and Therapeutics, University of Ibadan and University College Hospital, Ibadan.
[7]Institute for Advance Medical Research and Training, College of Medicine, University of Ibadan, Ibadan

[*]**Corresponding Author**:
Dr. Olalekan A. Agede
Email: agede.oa@unilorin.edu.ng

Peer-Review History
Received: 20 August 2022
Reviewed & Revised: 23/August/2022 to 18/September/2022
Accepted: 21 September 2022
Published: October 2022

Peer-Review Model
External peer-review was done through double-blind method.

ABSTRACT

Anti-malarial drugs such as chloroquine, Sulphadoxine-pyrimethamine and mefloquine have become ineffective in the treatment of malaria due to development of resistance by the malaria parasite. Consequently, the rise in defiance to older drugs initiated an emergency and a continuing need for the invention and development of novel antimalarial agents to treat vulnerable and drug-resistant burdens of malaria. A significant problem of malaria treatment and control is drug resistance procured by malaria parasites. one of the majorly examined enzymes in antimalarial drug composition due to its prospective role in Deoxyribonucleic acid (DNA) synthesis is Dihydrofolate Reductase (DHFR) in *Plasmodium falciparum* (PfDHFR- Thymidylate synthase (TS); TS refers to DHFR-linked thymidylate synthase in *Plasmodium falciparum*), which prompted the depletion of dihydrofolate to tetrahydrofolate. Hence, the purpose of this research aims to recognize prospective hits inhibiting DHFR and optimize them to the highest effectiveness and harmlessness in malaria treatment with a design strategy approach from the Chembl database, we procured Cycloguanil derivatives with biological activity data (pKi). The three-dimensional physicochemical captions of the compounds were computed. Quantitative structure-activity relationship (QSAR) model was constructed and a molecular mechanism was deduced by docking assay. Appertaining to the analysis, eleven (11) 3D descriptors were found to be accountable for pharmacological result related with Cycloguanil derivatives while hydrogen bonds were found to be ascribed to their strong binding affinities. The generated QSAR model was attested and found to be strong, which can be used to predict the action of novel compounds to the design of new antimalarials.

Keywords: Malaria, Lipophilic, QSAR model, DHFR, Cycloguanil

1. INTRODUCTION

Malaria is a parasitic disease transmitted by the bite of an infected female Anopheles mosquito. Usually, Malaria in humans is transmitted by five species of Plasmodium which are vivax, malariae, ovale, knowlesi and falciparum. Plasmodium falciparum happens to be the most common and causes severe and life-threatening disease [1]. *P.*

knowlesi is primarily monkey malaria parasite but causes human infection in forested regions of Southeast Asia [2]. This life-threatening disease happens to be a crucial health problem particularly in the developing world, killing about two million people each year. Antimalarials such as chloroquine, mefloquine, and Sulphadoxine-pyrimethamine have turned out to be inefficacious against the disease [3]. In 2001, the World Health Organization recommended treatment of malaria with combination therapy which could be artemisinin-based combination therapy or non-artemisinin based because of growing resistance to commonly used monotherapies such as chloroquine and sulfadoxine-pyrimethamine [4]. Recently, some reports from Southeast Asia and certain African countries revealed that there was reduced sensitivity and possible resistance of *P. falciparum* to artemisinin-based combination therapy [5-7]. Similar findings was also reported by TRAC study: tracking resistance to artemisinin collaboration; a multicenter study [8]. Therefore, for the treatment of Drug-susceptible and drug-resistant strains of malaria, the rise in resistance to earlier drugs have produced an emergency and continuing need for the invention and development of new antimalarial drugs. Cycloguanil is a dihydrofolate reductase inhibitor [9], and also a metabolite of the antimalarial drug proguanil (Figure 1). Its formation in vivo is thought to be mainly accountable for the antimalarial action of proguanil [10]. Although Cycloguanil is not presently in widespread use as an antimalarial drug, the ongoing development of resistance to current antimalarial drugs has led to renewed interest in studying the use of Cycloguanil in combination with other drugs [11].

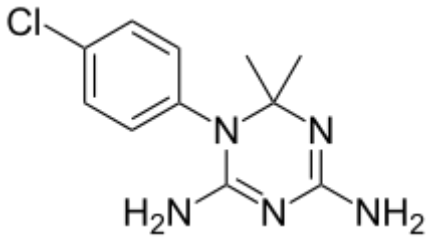

Figure 1: Structure of Cycloguanil

A paramount problem in the treatment and control of malaria is drug resistance acquired by malaria parasites. Dihydrofolate reductase (DHFR) in Pf (PfDHFR-TS; TS represent thymidylate DHFR-related synthase in Pf), which catalyzes the reduction of dihydrofolate to tetrahydrofolate is one of the majorly examined enzymes in the design of antimalarial drugs due to its possible role in DNA synthesis [12,13]. DHFR is also regarded as a competent target for other protozoan diseases such as leishmaniasis, trypanosomiasis and Chagas diseases [14]. Resistance of the parasite to antifolate is majorly caused by mutations at the functional site of the enzyme [15-17]. Certain number of the resistance-causing mutations comprise of a single S108N, double C59R+S108N, triple N51I+C59R+S108N, C59R+S108N+I164L and quadruple N51I+C59R+S108N+I164L. A double mutation, A16V+S108T, is distinct for resistance to the commercialized drug cycloguanil.

In recent years, several computational techniques have been implemented to effectively comprehend PfDHFR-TS-ligand interactions [18]. Researchers have developed homologous models to investigate the resistance mechanism of frequently used antifolate drugs prior to the release of the PfDHFR-TS crystal structures, [19]. In a previous study, molecular modeling studies were performed, as well as docking studies using GOLD program, to consider the chemical association between pyrimethamine derivatives and DHFR (PDBID: 1j3k structure). This was evaluated based on several scoring functions, including those of GOLD, Molegro virtual docker, Discovery Studio and MOE, and find the Molegro virtual docker protein-ligand interaction score to show good correlation with binding affinity data reported [20]. The same authors carried out binding studies of pyrimethamine derivatives in both wild-type and mutant enzymes [21]. The same authors also performed Structure-activity relationship (QSAR) studies using neural networks on this class of compounds [22]. QSAR studies for certain of the antifolates have been published [23]. Using Catalyst software on a varied set of PfDHFR-TS inhibitors, a 3D pharmacophore model was prepared, together with cycloguanil and pyrimethamine derivatives [24]. The Autodock program was also introduced to prognosticate the correct binding modes of folic acid competitive DHFR antagonists recognized using their cell-based high-throughput screening [25].

In summary, recent modeling studies concentrated on studying the interactions of different small molecules antagonists of DHFR with wild-type and mutant active-site residues using specific docking programs and 2D-QSAR studies. Nevertheless, new research is needed on the significance of 3D physicochemical properties with binding affinity data and on mechanistic insight based on protein-ligand interaction to examine molecular association precisely for this very fascinating and therapeutically salient class of compounds. Thus, our report includes two main objectives: (1) To quantitatively gain new knowledge about the relationship between structure-

activity (QSAR) based on 3D descriptors between wild-type and mutant-bound cycloguanil derivative type of PfDHFR-TS and (2) to understand the interaction mechanisms between PfDHFR-TS and cycloguanil derivatives.

2. MATERIALS AND METHODS

2.1. Collection of data and dataset groundwork

The trivial name, structure, origin and biological activities (Ki) of PfDHFR inhibitors were retrieved from ChEMBL database. A total of 62 PfDHFR inhibitors were recovered based on available chemical structures with correlated bioactivities (Ki) (Figure 2). Bioactivities (Ki) were then modified to pKi by adopting the expression pKi = (-log (Ki X)). The chemical structures of PfDHFR inhibitors were obtained from the ChEMBL database as smiles format, which was then changed to (3D) SDF format on DataWarrior v5.0.0. [26].

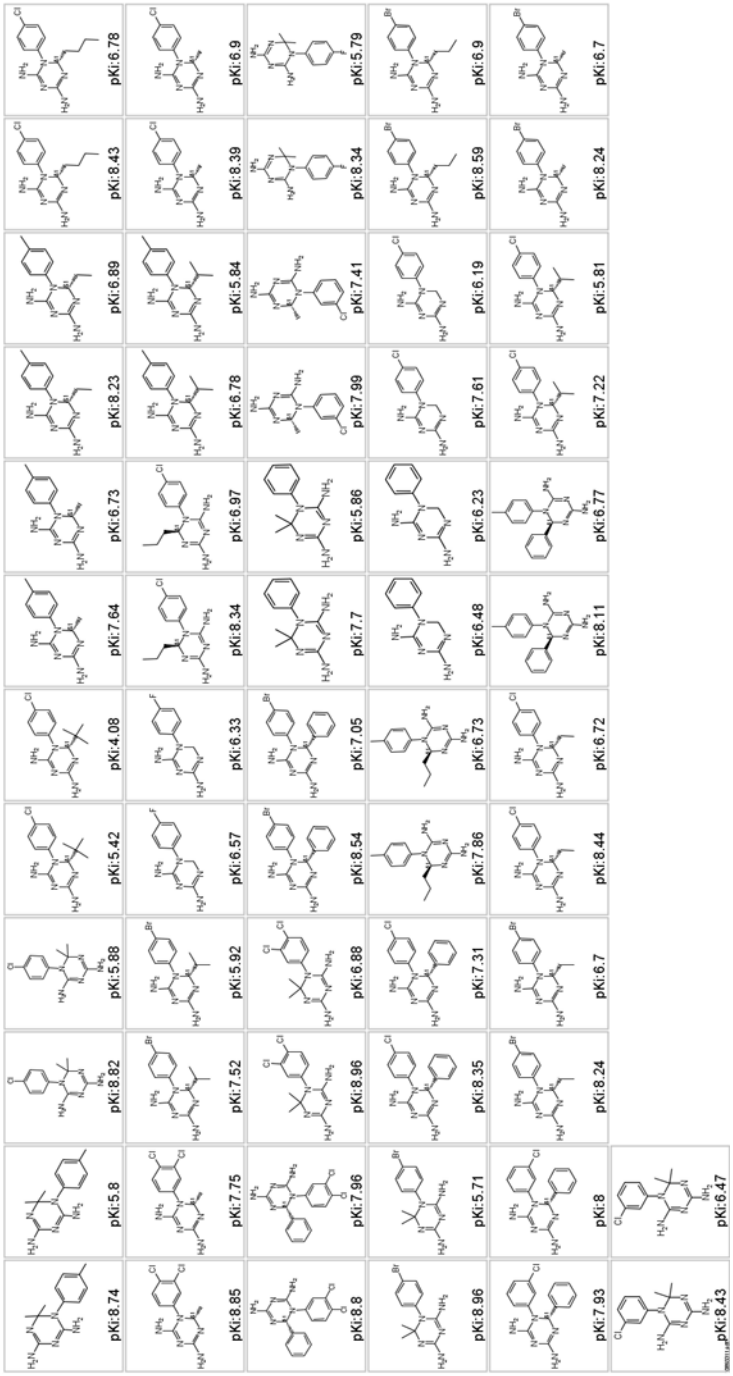

Figure 2: Raw data with corresponding bioactivities (pKi)

2.2. 3D-QSAR study

The effectiveness of a compound must be quantified with molecular descriptors in order to construct 3D- QSAR model [27] and hence, based on it, the online tool Chemopy [28] was adopted for calculation of different descriptors in the following groups: hybrid features, constitutional properties, electronic properties, topological properties, and geometric descriptions. The calculated properties were organized in matrix form. These calculated features were preprocessed to determine the correlation coefficient output of 0.99 based on the variance output 0.0001 and unchanged (fixed column) using JFrameVWSP version 1.0. The dataset of 62 molecules recovered from the literature [29] was splited for testing and training dataset by using the Kennard-Stone method [30].

QSAR model validation is necessary to assess how well founded a developed model is [31]. This is usually attained by assessing the internal firmness and prognostic potential of the QSAR models. In this study, the developed QSAR model was validated using the Leave-one-out (LOO) method to get the internal validation. This was done by removing one molecule, creating and validation of the model against a single molecule for all Q^2 (rCV^2) values and documented. Equation (1) was used to calculate the rCV^2 (cross-regression coefficient) to elucidate the internal firmness of the model.

$$rCV^2 = 1 - \frac{\sum\left(Y_{obs} - Y_{pred}\right)^2}{\sum\left(Y_{obs} - \overline{Y}\right)^2} \quad (1)$$

Where Y in the indicated equation represents the mean activity value of the training set. Y_{pred} and Y_{obs} represents the corresponding predicted and observed activity values. It is notable that an rCV greater than 0.5 indicates a realistically robust model [32].

After the internal validation process, the high predictive power of the QSAR model was screened by an external test set of compounds that were not applied to the QSAR model building. The predictive power or external validation achieved was determined based on the predictive R^2 (R_{pred}^2) in equation (2).

$$r^2_{prod} = 1 - \frac{\sum\left(Y_{pred(test)} - Y_{(test)}\right)^2}{\sum\left(Y_{(test)} - \overline{Y_{(training)}}\right)^2} \quad (2)$$

$Y_{(test)}$ and $Y_{pred(test)}$ is the observed activity and predicted values for test set compounds respectively.$Y_{(training)}$ is the average bioactivity of compound in the training set.

QSAR model (R_{pred}^2) greater than 0.6 is the acceptable predictive power for the test set molecules [27-29]. S-MLR method was used to develop QSAR model from the dataset to exam potential leads against PfDHFR inside a training dataset (48 compounds).

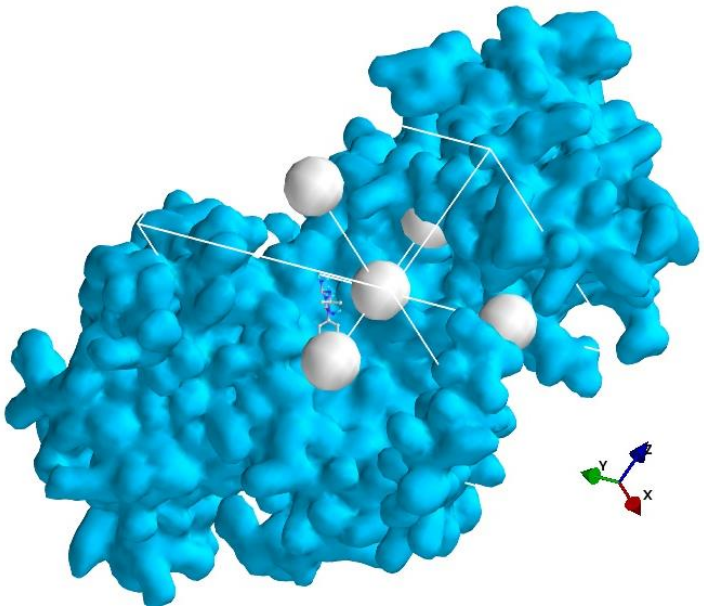

Figure 3: Grid box within which the Cycloguanil and derivatives binds

2.4 Molecular docking

The 3D crystal structure of (PDB: 3um6) from the Protein Database was obtained in Preparing the PfDHFR target. Discovery Studio 2017R2 was used to remove all heteroatoms while the Pymol tools for non-essential water molecules. Adjacent to receptor and ligands preparation, this study used the PyRx, AutoDock Vina option hinged on function scoring to carry out molecular docking analysis. PyRx, AutoDock Vina comprehensive docking mode for searching was used for analysis. After a successful minimization procedure, the analysis of the grid frame centered at 35.958 × 11.4079 × 38.1239 in the x, y, and z axes as appropriate for the grid Dimension 25x25x25 Å to indicate the binding site (Figure 3).

3. RESULTS AND DISCUSSION

To analyze the multiplicity of the testing and training set, the Principal Component Analysis approach (PCA) was adopted and the PCA was executed with structural descriptors evaluated for the entire data set. This approach helped to identify homogeneities in the total data, as well as to describe the spatial location of the samples to help in dividing the data into train and test sets.

Three principal components were revealed by the PCA results (PC1, PC2 and PC3), which accounted for 73.26% of all variables are as follows: PC1 = 37.809%, PC2 = 23.361% and PC3 = 12.09%. Since the first three principal components can explain most of the variability, the different score plot is a reliable example of the spatial distribution of scores for full evidence. The distribution of compounds in the initial space of the three principal components is as shown by the plot of PC1, PC2 and PC3 (Figure 4) that PC1 and PC2 cover the largest variation in overall data (Figure 5). This number revealed that the test samples and the training sets are uniformly distributed in 3D space, and consequently, the data set can be split. Additionally, the compounds in the training sets are represented across the entire data set.

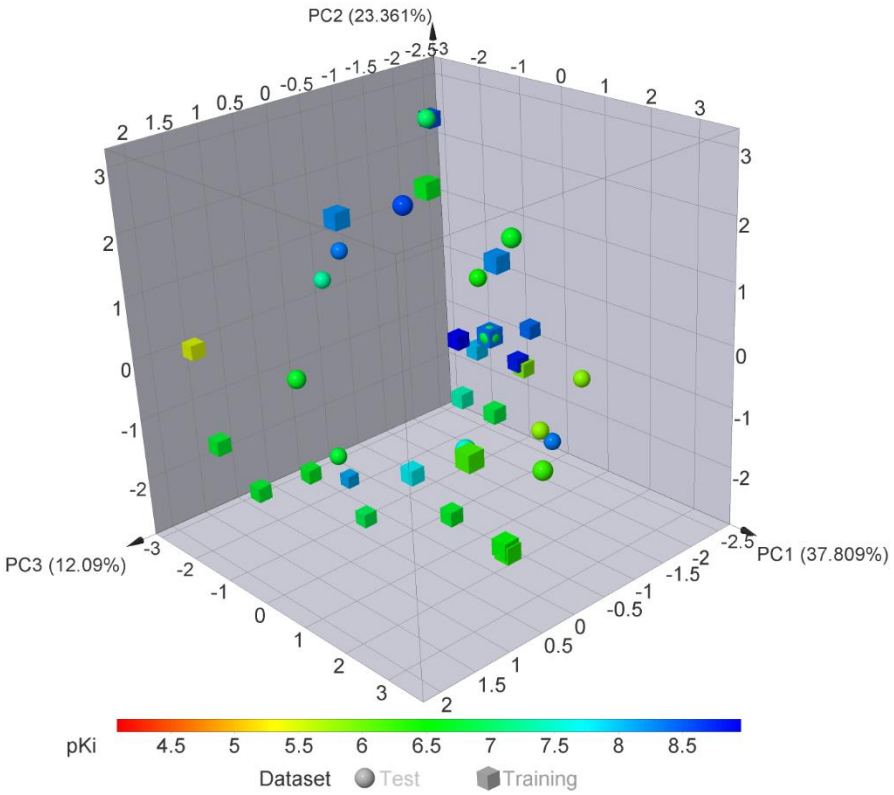

Figure 4: Analysis of the principal component of the test and train sets

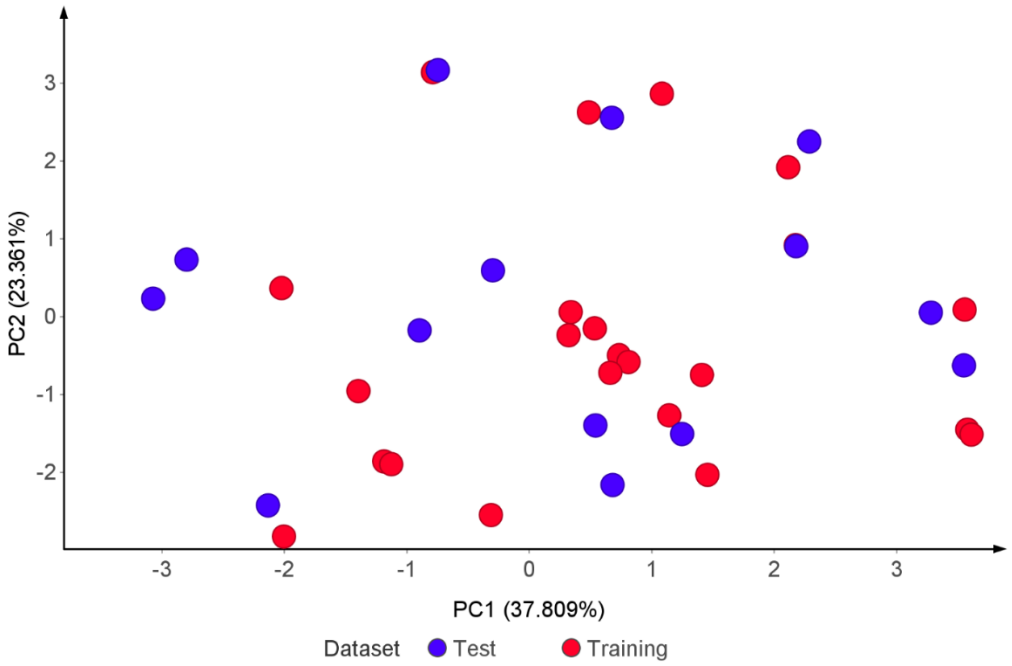

Figure 5: Analysis of principle component with PC1 and PC2

The next step after analysis was to split the data set into test and training set to identify and select the most important primary factors for DHFR inhibitory activity of the 62 cycloguanil derivatives. Stepwise-MLR (multiple linear regression) was applied as a variable selection method to select only the most important (relevant) combinations with them to obtain the model with maximum predictive power using a training data set. The eleven (11) most important descriptors in accordance with the S-MLR approach are P1e, MoRSEM6, P1m, MoRSEM30, RDFC6, RDFC5, RDFM11, RDFP7, MoRSEN20, MoRSEU2 and MoRSEM3 based on variance threshold of 0.01 and cross-correlation cut-off of 0.9. In this study, these Descriptors have been shown to be related to the biological response under study and are described in Figure 6.

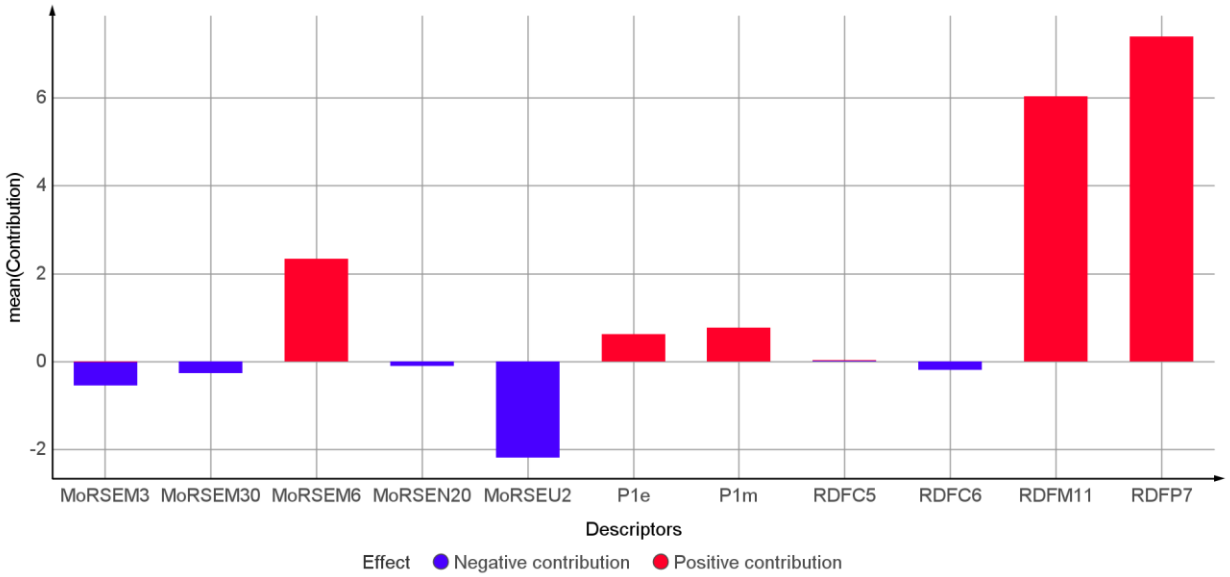

Figure 6: selected 3D-descriptors with their corresponding effects

Multiple Stepwise Linear Regression (S-MLR) analysis, using DTC Lab [36]. A stepwisefit function was applied and following the rules of significance statistical analysis, was applied to obtain the QSAR equation of interest. The addition or removal of a potential term to the test model was based on the p-value of the F statistic (Table 1). An Input tolerance of 0.05 and output tolerance of 0.10 was applied. Using leave-one-out cross-validation, the prognostic performance was assessed.

The QSAR equation describing pKi in terms of the selected 3D-descriptors is as follows:

pKi = -0.30975 + 1.19563 P1e - 0.03316 MoRSEM6 + 0.22044 P1m + 0.12332 MoRSEM30 - 0.1015 RDFC6 + 0.12174 RDFC5 -0.00327 RDFM11 + 0.00194 RDFP7 - 0.16778 MoRSEN20 + 0.00564 MoRSEU2- 0.00729 MoRSEM3

The above regression equation is statistically characterized by the square of the multiple correlation coefficient R^2 = 0.9984, MSE=0.00444, leave-one-out cross-validation Q^2 = 0.99681, See: 0.00553, SDEP (LOO):0.00666 and standard deviation in absolute errors (SD, 95% data):0.00294. The predictive power of the model is illustrated in Figure 7.

Table 1: S-MLR R2 based on each descriptor

Parameter	t-value	p-value	F-value	Stepwise-MLR R^2
P1e	38.88588	<0.0001	1512.11139	0.93649
MoRSEM6	-11.5027	<0.0001	132.312	0.98883
P1m	8.06027	<0.0001	64.96792	0.99245
MoRSEM30	6.55022	<0.0001	42.90545	0.99453
RDFC5	5.66283	<0.0001	32.0676	0.99537
RDFC6	-6.36169	<0.0001	40.47111	0.99636
RDFM11	-4.93637	0.00002	24.3678	0.99703
RDFP7	2.30092	0.02806	5.29423	0.99753
MoRSEN20	-3.35403	0.00206	11.24953	0.99784
MoRSEU2	3.00033	0.00519	9.00199	0.99815
MoRSEM3	-2.26043	0.03073	5.10953	0.9984
Adjusted R^2 = 0.99786				

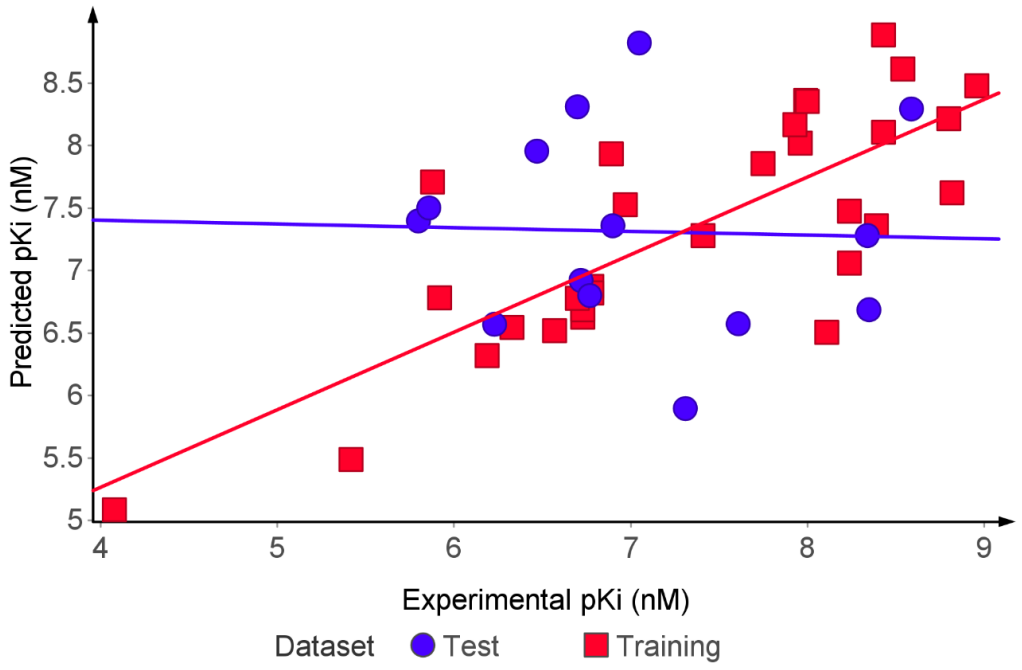

Figure 7: The predicted pKi values using MLR modeling against the experimental (observed) pIKi values

The built QSAR model, is statistically correct and easy to use for evaluation of pKi for any structurally defined compound sharing the same scaffold. Therefore, it can be applied to calculate the expected DHFR inhibitor potency of specific designed structure and decide whether or not it is worth of further considerations in the search for potential drugs.

The eleven descriptors for the finest model (S-MLR) used to derive the PC1–PC2 loading plots are shown in Figure 8. In terms of loads, it was confirmed that the compounds having a higher biological activity value on the right side show a greater effect on MoRSEM3, MoRSEN20, Descriptors MoRSEU2, Plm, RDFC6 and P1e are on the same side as in Figure 8. On the contrary, the compounds with lower biological activity values on the left side are of particular importance from RDFM11, RDFC5, RDFP7, MoRSEM6, and M0RSEM30.

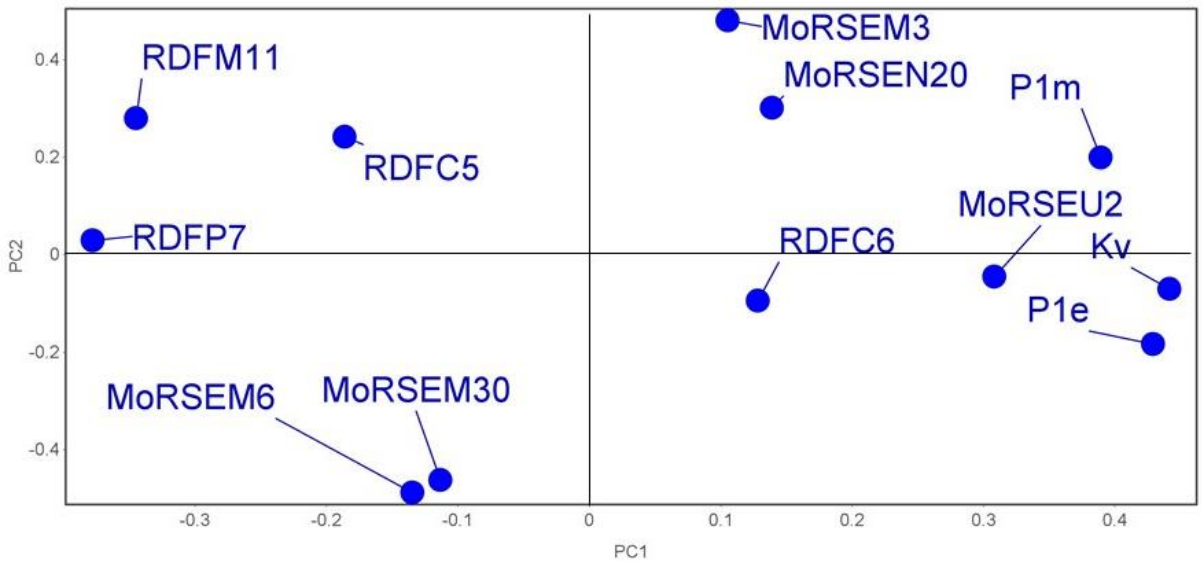

Figure 8: PC1–PC2 loadings plot using the eleven descriptors for the best model (S-MLR)

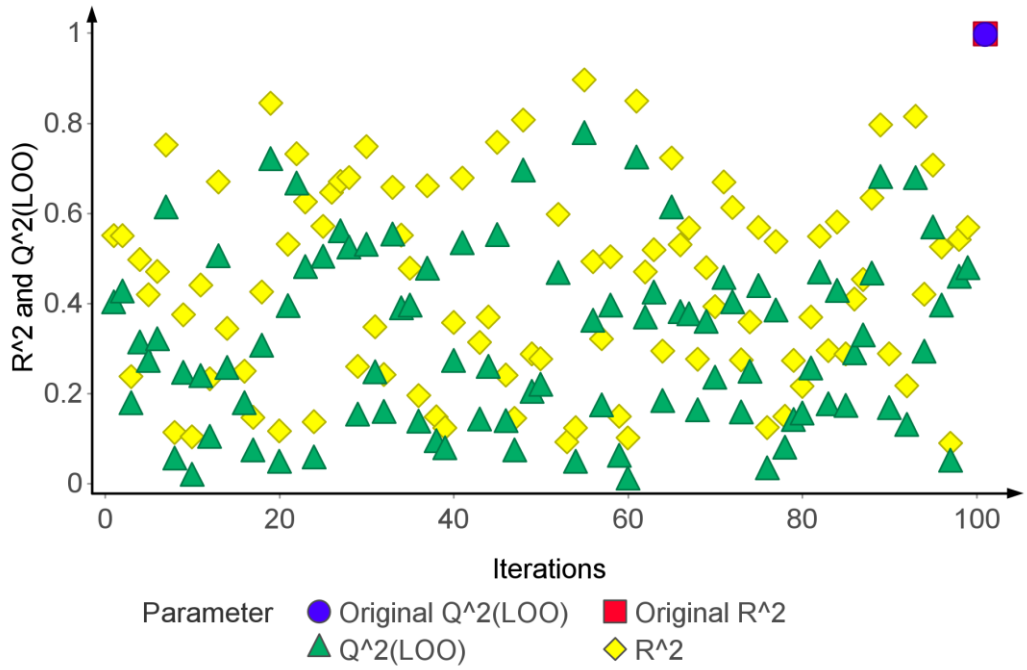

Figure 9: R^2 train and Q^2LOO values following numerous Y-randomization tests for S-MLR

The Y randomization test was performed to ensure that no random correlations were used in this study to validate the known QSAR model and also to ensure that the selected descriptors are not *accidental*. Therefore, the model results should be of low statistical quality. The generated MLR models were randomized by permuting the dependent variable while preserving the individual variables. The newly built QSAR models will be expected to have significantly low values of R^2 and Q^2 for more than a few experiments, thus confirming that the built QSAR models are robust. Approximately one hundred Y-randomization trials were performed. This study yielded lower values for R^2 and Q^2, thus validating the original model (the GA-MLR model was established) (Figure 9).

Residuals of predicted pKi values for training and testing versus experimental pKi values are plotted as shown in Figure 10. It was noticed that the model did not show relative and systematic error in general, since the spread of the residuals on the horizontal lines is random.

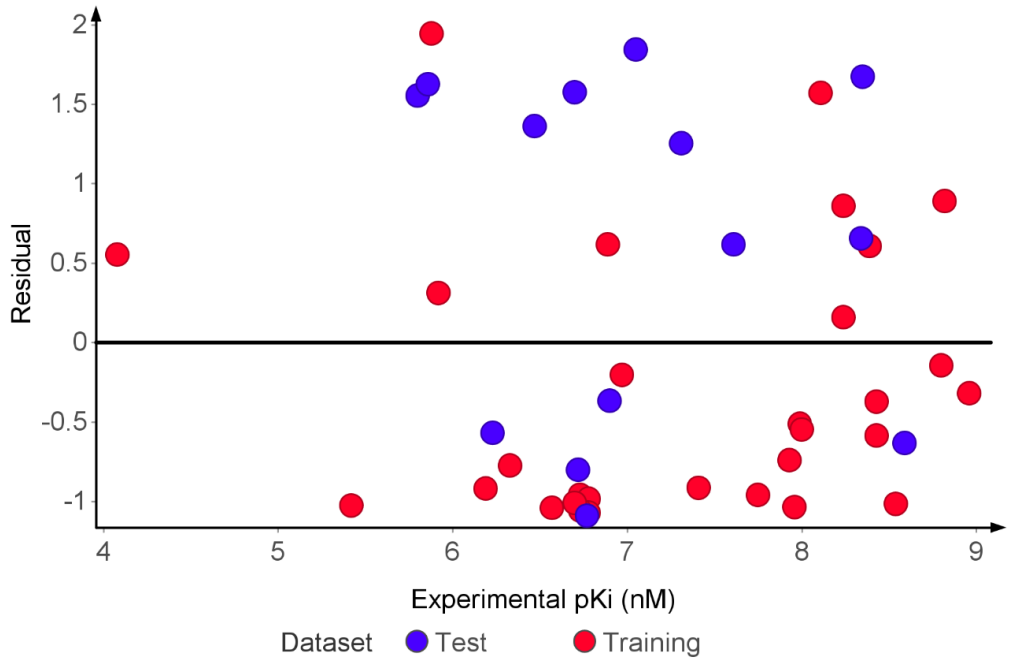

Figure 10: The residual against the experimental pKi by adopting S-MLR

Molecular docking was used in this study in order to better understand the molecular mechanism fundamental to the action of cycloguanil derivatives against DHFR. In the present study, the 62 cycloguanil derivatives and a co-crystallizing ligand for DHFR (PDBID:1CY), a molecule docked in the binding pocket of DHFR for its inhibitor (antagonist) activities. Six compounds manifested better binding affinity than the standard ligand (co - crystallized ligand), where 149732 and 149235 have the highest binding affinity of -7.2 kcal/mol, compared to the standard molecule (PDBID; -6.0 kcal/mol) and are therefore considered as the hit compounds (Table 2).

Table 2: Binding affinities of cycloguanil derivatives with the highest docking score

Ligand (CHEMBL ID)	Binding Affinity (kcal/mol)
149732	-7.2
149235	-7.2
149759	-6.9
150373	-6.8
149866	-6.8
149843	-6.7
Standard	-6.0

The highest binding energy of -7.2 kcal/mol attributed to 149732 is believed to result from chemical interactions in the receptor active site (Figure 11a) comprising: five (5) hydrogens bonds involving LYS359 residues, TYR322, and ASP212. Two (2) hydrophobic interactions involving PR0324 and LYS359 residues (Fig. 11b and c, Table 3).

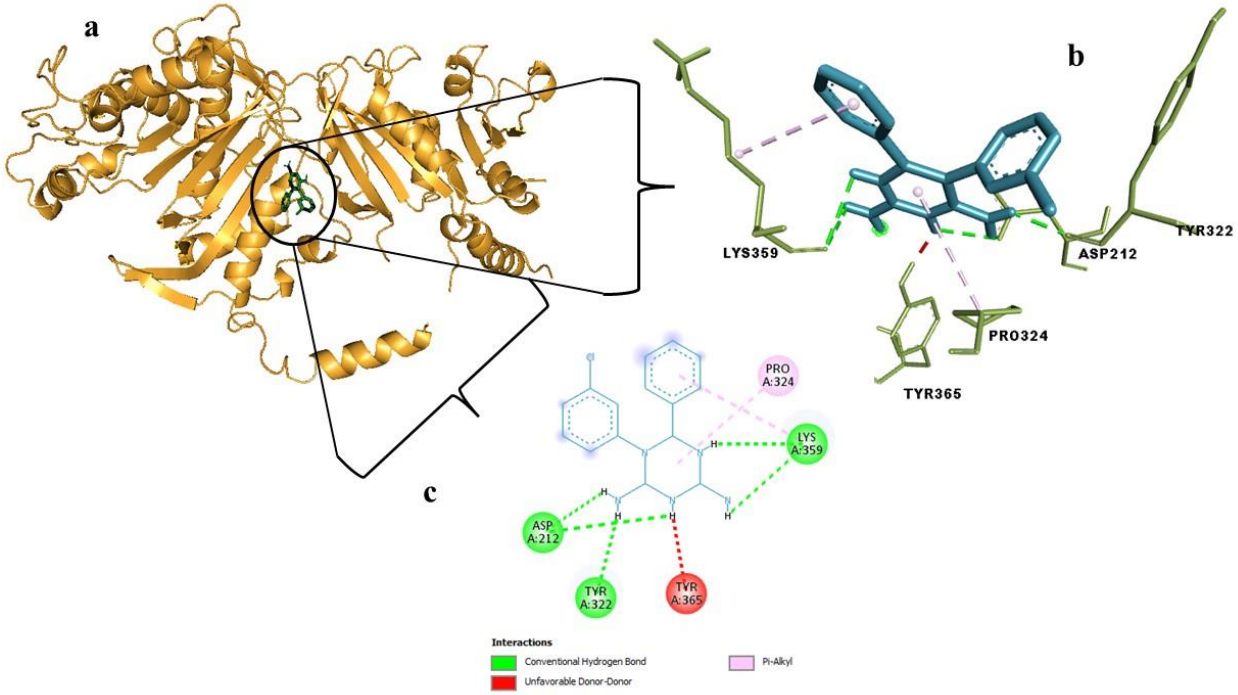

Figure 11: (a) DHFR binding pocket within which the cycloguanil derivatives bind (b) 2D- and (c) 3D-interaction between 149732 and DHFR

Table 3: Chemical interaction table between the atoms of 149732 and DHFR binding residues

Name	XYZ:X	XYZ: Y	XYZ: Z	Bond Distance	Category
N:LIGAND:H - A:TYR322:O	31.8015	6.1775	36.1515	2.12763	Hydrogen Bond
N:LIGAND:H - A:ASP212:OD1	30.2745	8.398	36.9865	1.93859	Hydrogen Bond
N:LIGAND:H - A:LYS359:O	29.0625	11.241	31.525	2.98257	Hydrogen Bond
N:LIGAND:HN - A:ASP212:OD1	29.705	9.152	36.406	2.96375	Hydrogen Bond
N:LIGAND:HN - A:LYS359:O	29.314	10.2865	30.9465	2.90736	Hydrogen Bond
N:LIGAND - A:PRO324	31.2421	9.15758	34.6303	5.16227	Hydrophobic
N:LIGAND - A:LYS359	28.2071	8.591	28.2365	4.54188	Hydrophobic

By accelerating molecular interactions, hydrogen (H) bonds enhance a variety of cellular functions. In other words, hydrogen bonds are thought to aid protein-ligand binding [37, 38]. Previous studies have revealed that receptor-ligand H binding pairs are interdependent, high affinity binding, corresponding to an increase in binding affinity [39].

4. CONCLUSION

We were able to produce a reliable QSAR model that described the biological activity markers *in vitro* of cycloguanil derivatives from a physicochemical calculation. Observed and the predicted data distribution was taken into account by the widely generated relationship range of numeric data. Therefore, it appears that a reliable estimate of biological activity can be made for each cycloguanil derivative which is structurally defined to rationally guide the search for the best possible DHFR inhibitor drugs.

Funding

This study has not received any external funding.

Conflicts of interests

The authors declare that there are no conflicts of interests.

Data and materials availability

All data associated with this study are present in the paper.

REFERENCES AND NOTES

1. Dhingra, V., Rao, K. V., & Narasu, M. L. (1999). Current status of artemisinin and its derivatives as antimalarial drugs. *Life sciences*, *66*(4), 279-300.
2. Guidelines for the Treatment of Malaria. World Health Organization; 2015 http://www.who.int/malaria/publications/atoz/who-guidelines-treatment-malaria-tmih-2015. (Accessed 14th May 2022)
3. Jamaludin, R., & Hasan, M. N. (2010). Quantitative structure-activity relationship for antimalarial activity of artemisinin. *Malaysian Journal of Fundamental and Applied Sciences*, *6*(1).
4. World Health Organization. Guidelines for the treatment of malaria, 2nd edition. http://www.who.int/malaria/publications/atoz/who-guidelines-treatment-malaria-tmih-2014. (Accessed 14th May 2022)
5. Kavishe RA, Paulo P, Kaaya RD, Kalinga A, van Zwetselaar M, Chilongola J, et al. Surveillance of artemether-lumefantrine associated Plasmodium falciparum multidrug resistance protein-1 gene polymorphisms in Tanzania. Malar J. 2014; 13(1):264-70.
6. Betson M, Sousa-Figueiredo JC, Atuhaire A, Arinaitwe M, Adriko M, Mwesigwa G, et al. Detection of persistent Plasmodium spp. infections in Ugandan children after artemether-lumefantrine treatment. Parasitology. 2014; 141(14):1880–90.
7. Wongsrichanalai C, Meshnick SR. Declining artesunate-mefloquine efficacy against falciparum malaria on the Cambodia-Thailand border. Emerg Infect Dis. 2008; 14(5):716–9.
8. Ashley EA, Dhorda M, Fairhurst RM, Amaratunga C, Lim P, Suon S, et al. Spread of artemisinin resistance in Plasmodium falciparum malaria. N Engl J Med. 2014; 371:411–23.
9. Srivastava, I. K., & Vaidya, A. B. (1999). A mechanism for the synergistic antimalarial action of atovaquone and proguanil. *Antimicrobial agents and chemotherapy*, *43*(6), 1334-1339.
10. Watkins, W. M., Sixsmith, D. G., & Chulay, J. D. (1984). The activity of proguanil and its metabolites, cycloguanil and p-chlorophenylbiguanide, against Plasmodium falciparum in vitro. *Annals of Tropical Medicine & Parasitology*, *78*(3), 273-278.
11. Walzer, P. D., Foy, J., Steele, P., & White, M. (1993). Synergistic combinations of Ro 11-8958 and other dihydrofolate reductase inhibitors with sulfamethoxazole and dapsone for therapy of experimental pneumocystosis. *Antimicrobial agents and chemotherapy*, *37*(7), 1436-1443.
12. Gregson, A., & Plowe, C. V. (2005). Mechanisms of resistance of malaria parasites to antifolates. *Pharmacological reviews*, *57*(1), 117-145.
13. Kompis, I. M., Islam, K., & Then, R. L. (2005). DNA and RNA synthesis: antifolates. *Chemical reviews*, *105*(2), 593-620.
14. Gilbert, I. H. (2002). Inhibitors of dihydrofolate reductase in Leishmania and trypanosomes. *Biochimica et Biophysica Acta (BBA)-Molecular Basis of Disease*, *1587*(2-3), 249-257.
15. Anderson, A. C. (2005). Targeting DHFR in parasitic protozoa. *Drug discovery today*, *10*(2), 121-128.
16. Hyde, J. E. (1990). The dihydrofolate reductase-thymidylate synthetase gene in the drug resistance of malaria parasites. *Pharmacology & therapeutics*, *48*(1), 45-59.
17. Yuthavong, Y., Yuvaniyama, J., Chitnumsub, P., Vanichtanankul, J., Chusacultanachai, S., Tarnchompoo, B., ... & Kamchonwongpaisan, S. (2005). Malarial (Plasmodium falciparum) dihydrofolate reductase-thymidylate synthase: structural basis for antifolate resistance and development of effective inhibitors. *Parasitology*, *130*(3), 249-259.
18. Adane, L., & Bharatam, P. V. (2008). Modelling and informatics in the analysis of P. falciparum DHFR enzyme inhibitors. *Current medicinal chemistry*, *15*(16), 1552-1569.
19. Delfino, R. T., Santos-Filho, O. A., & Figueroa-Villar, J. D. (2002). Molecular modeling of wild-type and antifolate resistant mutant Plasmodium falciparum DHFR. *Biophysical chemistry*, *98*(3), 287-300.
20. Fogel, G. B., Cheung, M., Pittman, E., & Hecht, D. (2008). Modeling the inhibition of quadruple mutant Plasmodium falciparum dihydrofolate reductase by pyrimethamine derivatives. *Journal of Computer-Aided Molecular Design*, *22*(1), 29-38.
21. Fogel, G. B., Cheung, M., Pittman, E., & Hecht, D. (2008). In silico screening against wild-type and mutant Plasmodium falciparum dihydrofolate reductase. *Journal of Molecular Graphics and Modelling*, *26*(7), 1145-1152.
22. Hecht, D., Cheung, M., & Fogel, G. B. (2008). QSAR using evolved neural networks for the inhibition of mutant

PfDHFR by pyrimethamine derivatives. *Biosystems*, *92*(1), 10-15.

23. Santos-Filho, O. A., & Hopfinger, A. J. (2001). A search for sources of drug resistance by the 4D-QSAR analysis of a set of antimalarial dihydrofolate reductase inhibitors. *Journal of computer-aided molecular design*, *15*(1), 1-12.
24. Parenti, M. D., Pacchioni, S., Ferrari, A. M., & Rastelli, G. (2004). Three-dimensional quantitative structure− activity relationship analysis of a set of Plasmodium falciparum dihydrofolate reductase inhibitors using a pharmacophore generation approach. *Journal of medicinal chemistry*, *47*(17), 4258-4267.
25. Plouffe, D., Brinker, A., McNamara, C., Henson, K., Kato, N., Kuhen, K., ... & Winzeler, E. A. (2008). In silico activity profiling reveals the mechanism of action of antimalarials discovered in a high-throughput screen. *Proceedings of the National Academy of Sciences*, *105*(26), 9059-9064.
26. O'Boyle, N.M., Banck, M., James, C.A., Morley, C., Vandermeersch, T. and Hutchison, G.R., 2011. Open Babel: An open chemical toolbox. *Journal of cheminformatics*, *3*(1), p.33.
27. Mahabeleshwar, G.H. and Kundu, G.C., 2003. Tyrosine kinase p56lck regulates cell motility and nuclear factor κB-mediated secretion of urokinase type plasminogen activator through tyrosine phosphorylation of IκBα following hypoxia/reoxygenation. *Journal of Biological Chemistry*, 278(52), pp.52598-52612.
28. Cao, D. S., Xu, Q. S., Hu, Q. N., & Liang, Y. Z. (2013). ChemoPy: freely available python package for computational biology and chemoinformatics. *Bioinformatics*, 29(8), 1092-1094.
29. Yuthavong, Y., Vilaivan, T., Chareonsethakul, N., Kamchonwongpaisan, S., Sirawaraporn, W., Quarrell, R., & Lowe, G. (2000). Development of a lead inhibitor for the A16V+ S108T mutant of dihydrofolate reductase from the cycloguanil-resistant strain (T9/94) of Plasmodium falciparum. *Journal of medicinal chemistry*, *43*(14), 2738-2744.
30. Paul, M.K. and Mukhopadhyay, A.K., 2004. Tyrosine kinase–role and significance in cancer. *International journal of medical sciences*, *1*(2), p.101.
31. Roy, K., Das, R.N., Ambure, P. and Aher, R.B., 2016. Be aware of error measures. Further studies on validation of predictive QSAR models. *Chemometrics and Intelligent Laboratory Systems*, *152*, pp.18-33.
32. Veber, D.F., Johnson, S.R., Cheng, H.Y., Smith, B.R., Ward, K.W. and Kopple, K.D., 2002. Molecular properties that influence the oral bioavailability of drug candidates. *Journal of medicinal chemistry*, *45*(12), pp.2615-2623.
33. Yadav, D.K. and Khan, F., 2013. QSAR, docking and ADMET studies of camptothecin derivatives as inhibitors of DNA topoisomerase-I. *Journal of Chemometrics*, *27*(1-2), pp.21-33.
34. Yadav, D.K., Kumar, S., Saloni, H.S., Kim, M.H., Sharma, P., Misra, S. and Khan, F., 2017. Molecular docking, QSAR and ADMET studies of withanolide analogs against breast cancer. *Drug Design, Development and Therapy*, *11*, p.1859.
35. Kumar Yadav, D., Kalani, K., Khan, F. and Kumar Srivastava, S., 2013. QSAR and docking based semi-synthesis and in vitro evaluation of 18 β-glycyrrhetinic acid derivatives against human lung cancer cell line A-549. *Medicinal Chemistry*, *9*(8), pp.1073-1084.
36. Mackert, M., Guadagno, M., Mabry, A., & Chilek, L. (2013). DTC drug advertising ethics: Laboratory for medical marketing. *International Journal of Pharmaceutical and Healthcare Marketing*.
37. Salentin, S., Haupt, V.J., Daminelli, S. and Schroeder, M., 2014. Polypharmacology rescored: Protein–ligand interaction profiles for remote binding site similarity assessment. *Progress in biophysics and molecular biology*, *116*(2-3), pp.174-186.
38. Sawada, T., 2012. Chemical insight into the influenza a virus hemagglutinin binding to the sialoside revealed by the fragment molecular orbital method. *Open Glycoscience*, *5*(1).
39. Chen, D., Oezguen, N., Urvil, P., Ferguson, C., Dann, S.M. and Savidge, T.C., 2016. Regulation of protein-ligand binding affinity by hydrogen bond pairing. *Science advances*, *2*(3), p.e1501240.